Upper critical fields and two-band superconductivity in $Sr_{1-x}Eu_x(Fe_{0.89}Co_{0.11})_2As_2$ ($x = 0.20$ and 0.46)

Rongwei Hu,[1,*] Eun Deok Mun,[2] M. M. Altarawneh,[2,†] C. H. Mielke,[2] V. S. Zapf,[2] S. L. Bud'ko,[1] and P. C. Canfield[1]

[1]*Ames Laboratory, US Department of Energy and Department of Physics and Astronomy, Iowa State University, Ames, Iowa 50011, USA*

[2]*National High Magnetic Field Laboratory, Los Alamos National Laboratory, Los Alamos, New Mexico 87545, USA*

(Received 29 November 2011; published 13 February 2012)

The upper critical fields $H_{c2}(T)$ of single crystals of $Sr_{1-x}Eu_x(Fe_{0.89}Co_{0.11})_2As_2$ ($x = 0.20$ and 0.46) were determined by radio-frequency penetration depth measurements in pulsed magnetic fields. $H_{c2}(T)$ approaches the Pauli limiting field but shows an upward curvature with an enhancement from the orbital limited field, as inferred from the Werthamer-Helfand-Hohenberg theory. We discuss the temperature dependence of the upper critical fields and the decreasing anisotropy using a two-band BCS model.

DOI: 10.1103/PhysRevB.85.064511 PACS number(s): 74.25.Op, 74.25.Dw, 74.70.Dd

I. INTRODUCTION

The upper critical field $H_{c2}(T)$ and its anisotropy are fundamental characteristics of a type-II superconductor; they provide information about the underlying electronic structure and can shed light on the mechanism of Copper pair breaking. Therefore, both for the understanding of superconductivity and potential application, extensive studies of $H_{c2}(T)$ have been performed on the recently discovered FeAs-based superconductors. Large upper critical fields have been observed for FeAs superconductors.[1–7] More interestingly, some of their $H_{c2}(T)$ exhibit pronounced upward curvature of $H_{c2}(T)$, implying a multiband nature of superconductivity.[5,8–10] In contrast to the high T_c cuprates with their very large anisotropy, measurements of $H_{c2}(T)$ of the FeAs superconductors have revealed that the anisotropic ratio $\gamma = H_{c2}^{ab}/H_{c2}^{c}$ decreases with decreasing temperature and becomes nearly isotropic at low temperatures for the 122 and 111 type of FeAs materials.[6–8,11]

The previous study of Eu-doped $Sr(Fe_{0.88}Co_{0.12})_2As_2$ demonstrated the interaction between the FeAs-based superconductivity and magnetism due to Eu^{2+}: in the disordered paramagnetic region of Eu^{2+}, superconductivity is weakly suppressed by spin-flip scattering associated with the local magnetic moments of Eu^{2+}; it is further suppressed with developing long-range antiferromagnetic order of Eu^{2+} and coexists with antiferromagnetism of Eu^{2+} as long as $T_c > T_N$.[12] It is of great interest to see how the superconductivity is affected by the magnetism of Eu^{2+} by mapping out the H-T phase diagram.

Moreover, in the study of the interplay of superconductivity and magnetism, it is proposed by Jaccarino and Peter[13] that for certain rare-earth-bearing intermetallics, the external magnetic field, which in general inhibits superconductivity, may be canceled by the effective exchange field $H_{\rm eff}$ of the magnetic moments, imposed on the conduction electrons, when $H_{\rm eff}$ is opposite to the direction of the applied field. Therefore, superconductivity can occur in two domains: one at the low field, where the pair-breaking field is still small, and one at the high field in the compensation region. Experimentally, an anomalous enhancement of $H_{c2}(T)$ was first reported by Fischer *et al.*[14] in $Sn_{1.2(1-x)}Eu_xMo_{6.35}S_8$ and $Pb_{1-x}Eu_xMo_{6.35}S_8$ chevrel phases. Attributed to this "Jaccarino-Peter" effect, magnetic-field-induced superconductivity in the H_{c2}-T phase diagram was indeed observed in $Eu_{0.75}Sn_{0.25}Mo_6S_{7.2}Se_{0.8}$ and fitted well with the Jaccarino-Peter scenario.[15] Therefore, the properties of $Sr_{1-x}Eu_x(Fe_{0.89}Co_{0.11})_2As_2$, as possible candidates for observation of the Jaccarino-Peter effect, are worth investigating.

In this paper, we report the upper critical fields of $Sr_{1-x}Eu_x(Fe_{0.89}Co_{0.11})_2As_2$ ($x = 0.20$ and 0.46) single crystals determined by radio-frequency, contactless, penetration depth measurements. The two selected samples are the representative concentrations in the disordered paramagnetic region and coexistence region of superconductivity and antiferromagnetism. We find that for both concentrations, the curves of $H_{c2}(T)$ can be consistently explained by the two-band model, and the anisotropy decreases with temperature, approaching an isotropic state at low temperatures.

II. EXPERIMENT

Single crystals of $Sr_{1-x}Eu_x(Fe_{0.89}Co_{0.11})_2As_2$ were grown from self-flux, similar to that in Ref. 12. But the annealing procedure is different from the previous one. After FeAs flux was decanted, sample ampules were annealed at 500 °C for 24 hours before opening. Thus, the air exposure of the crystals was minimized. The chemical composition was determined by wavelength dispersive x-ray spectroscopy (WDS) in a JEOL JXA-8200 electron microscope. The magnetic susceptibility was measured in a Quantum Design, Inc. Magnetic Property Measurement System (MPMS). The temperature and magnetic field dependences of the electrical resistance were measured using the four probe ac ($f = 16$ Hz) technique in a Quantum Design, Inc. Physical Property Measurement System (PPMS). Radio-frequency (rf), contactless, penetration depth measurements were performed on the single-crystal sample in a 60 T pulsed-field magnet with a 10 ms rise time and a 40 ms extended decay. The rf technique is highly sensitive to small changes (∼1–5 nm) in the rf penetration depth, thus it is an accurate method for determining the upper critical field in anisotropic superconductors.[16] Small single crystals were selected because of the eddy current heating in the pulsed field. To determine the upper critical-field anisotropy, the single crystal was measured in two configurations, $H \parallel ab$ and $H \parallel c$. More details about this technique can be found in Refs. 4, 17, and 18.

III. RESULTS AND DISCUSSIONS

The actual compositions of the two samples determined by WDS were $Sr_{0.797}Eu_{0.203}(Fe_{0.888}Co_{0.112})_2As_2$ and $Sr_{0.537}Eu_{0.463}(Fe_{0.885}Co_{0.115})_2As_2$. For brevity, we denote them as the Eu20 and Eu46 sample in the following text. The Co concentrations are close to the optimal doping, $x \sim 0.12$, for $Sr(Fe_{1-x}Co_x)_2As_2$, as in Ref. 12. Figure 1(a) shows the low-temperature magnetic susceptibility and resistivity of the two samples. Since we are measuring the in-plane magnetic susceptibility and the sample is a thin platelike one, with an aspect ratio (in-plane dimension/thickness) of more than 10, the demagnetization factor is negligibly small (less than 0.05).[19] The large diamagnetic shielding indicates bulk superconductivity. The superconducting transition temperatures inferred from the first deviation point from the normal magnetic susceptibility of the zero-field-cooled curve are 18 and 16.2 K for Eu20 and Eu46, respectively. The Eu46 sample shows a weak anomaly due to antiferromagnetic ordering of Eu^{2+} at 3.5 K, indicated in the inset of Fig. 1(a), as that in Ref. 12. The T_c in resistivity, as inferred by extrapolating the steepest slope to zero resistance, are 18.3 and 16.8 K for the two samples, which is in agreement

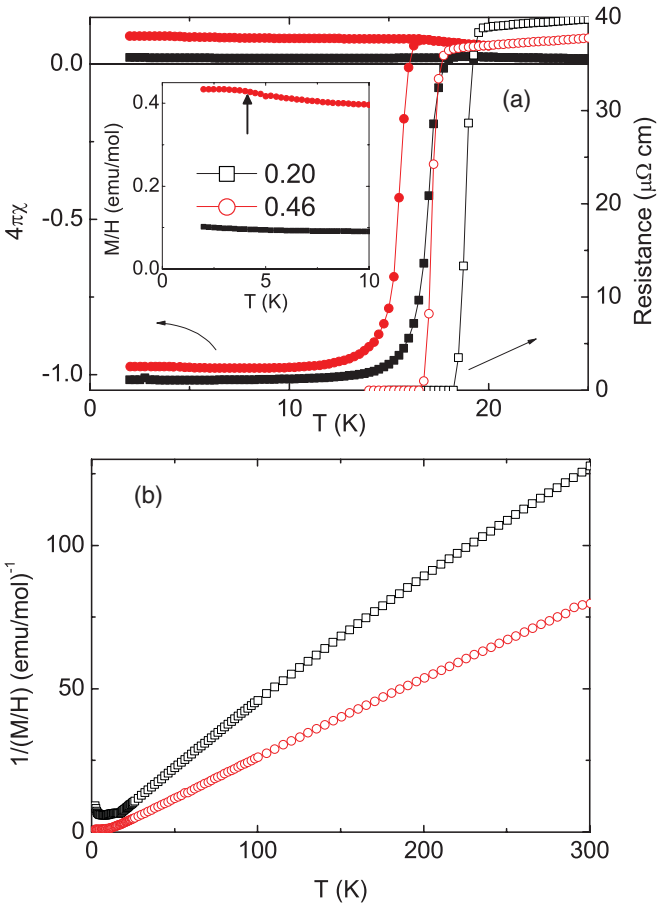

FIG. 1. (Color online) (a) Low-temperature magnetic susceptibility measured in a magnetic field of 100 Oe applied in the *ab* plane and resistivity in the zero field. The inset shows an expanded view of the field-cooled curve. The arrow indicates the antiferromagnetic transition. (b) Inverse in-plane magnetic susceptibility measured in 10 kOe.

with the magnetic-susceptibility measurements. The inverse in-plane magnetic susceptibility measured in 10 kOe of the two samples is plotted in Fig. 1(b). The Curie-Weiss fits above 150 K give an estimated Eu concentration of 0.22 and 0.47 by assuming 7.94 μ_B/Eu^{2+} ion. Thus, all of the above observations are consistent with those in Ref. 12, and show that Eu20 is in the disordered paramagnetic region of Eu^{2+} and Eu46 is in the coexistence region of superconductivity and antiferromagnetism. This being said, we should note that the T_c values of the present samples are 6–7 K higher than those in Ref. 12. This is most likely due to the difference in heat treatment and also may be due to a slight shift in the Co concentrations. Fortunately, given the robust nature of Eu^{2+} magnetism, this shift in T_c does not adversely effect our goal of studying the effects of local-moment magnetism on $H_{c2}(T)$.

The frequency shift as a function of the magnetic field applied parallel and perpendicular to the *ab* plane at different temperatures from 1.5 to 19 K for Eu20 is shown in Fig. 2. The normal state has a smooth and nearly linear field dependence as manifested by the 19 K curve.[20] H_{c2} is identified as the point at which the slope of the ΔF intercepts the normal-state background of 19 K. Other criterion, e.g., the first point deviating from the normal-state background, can be used and the difference between these two criteria is taken as the error bar for $H_{c2}(T)$. For $H \parallel c$ in Fig. 2(b), the sample has a weaker coupling to the detection coil, resulting in a smaller but still easily resolvable frequency shift. The same rf measurements are performed on the Eu46 sample for both orientations for temperatures down to 0.51 K, as is shown in Fig. 3. In the previous study in Ref. 12, it was shown that the Eu^{2+} moments undergo a metamagnetic transition from antiferromagnetic to ferromagnetic above a magnetic field of 4 kOe. Thus, it behaves as a superconductor with ferromagnetically coupled Eu^{2+} moments at the low-temperature high field. In order to look for a possible Jaccarino-Peter effect, the frequency shift of the Eu46 sample was measured in a field up to 60 T at the base temperature 0.51 K for both directions [see inset in Fig. 3(b)]. No anomaly associated with superconductivity can be observed in high fields. So either the magnetic field is still too low to compensate the exchange field, or the exchange field has the same sign as the external field and no cancellation is realized.

Figure 4 shows the $H_{c2}(T)$ curves for $H \parallel ab$ (H_{c2}^{ab}) and $H \parallel c$ (H_{c2}^{c}) for both samples. For the Eu20 sample, $H_{c2}^{ab}(T)$ is almost linear close to T_c, which is a traditional Werthamer-Helfand-Hohenberg (WHH) behavior, but $H_{c2}^{c}(T)$ exhibits a significant upward curvature. This negative curvature is even more pronounced for the Eu46 sample in Fig. 4(b) for both field orientations. The dashed lines in Fig. 4 are fits to the conventional one-band WHH theory.[21] The $H_{c2}(T)$ values from direct measurements are far above the prediction of the WHH theory, except for the $H \parallel ab$ curve of the Eu20 sample (see later discussion). The other mechanism for limiting $H_{c2}(T)$ is the Pauli spin paramagnetic effect as a result of the Zeeman effect exceeding the condensation energy of Copper pairs, given by $\mu_0 H_p = 1.84 T_c$ for isotropic *s*-wave pairing in the weak-coupling limit.[22] $\mu_0 H_p$ is estimated to be 30.9 and 29.4 T for Eu20 and Eu46, respectively. These values are close to the experimental results extrapolated to 0 K, implying that the Pauli paramagnetic effect might be the dominant

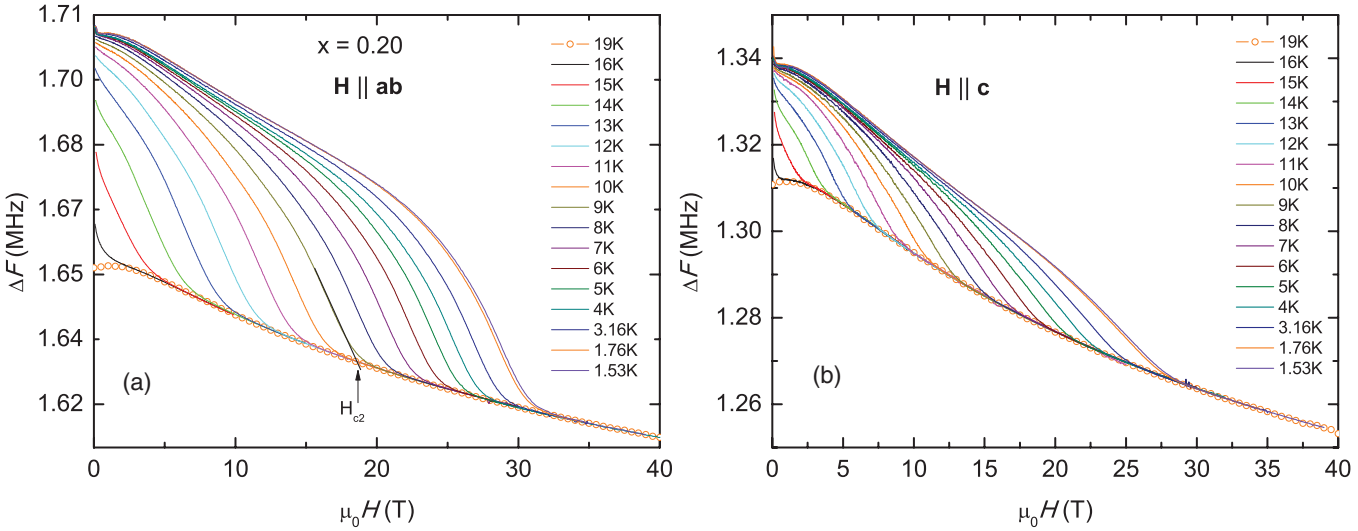

FIG. 2. (Color online) Frequency shift (ΔF) as a function of magnetic field for $H \parallel ab$ and $H \parallel c$ for the Eu20 sample at selected temperatures. Open symbols are ΔF taken at 19 K as a normal-state background signal. Solid line in (a) shows the criterion used to determine $H_{c2}(T)$.

pair-breaking mechanism for limiting the upper critical fields in these compounds. It is worth noting that for the $x = 0.46$ sample, the magnitude of $H_{c2}(T)$ is reduced and its curvature is changed. This is not unexpected given the rough doubling of local-moment-bearing Eu^{2+}, which manifests very nonlinear $M(H)$ behavior.[12]

The anomalous upward curvature of $H_{c2}(T)$ has been observed in other multiband systems such as MgB_2,[23] and recently in FeAs superconductors, e.g., $Ba(Fe_{0.9}Co_{0.1})_2As_2$,[5] $LaFeAsO_{0.89}F_{0.11}$,[8] $NdFeAsO_{0.7}F_{0.3}$,[9] and $Sr(Fe_{0.9}Co_{0.1})_2As_2$ thin film,[10] and explained within a two-band BCS model by taking into account the inter- and intraband scattering in $H_{c2}(T)$.[23] In the two-band s-wave theory, the intra- and interband interactions are described by a 2×2 matrix of the BCS coupling constants λ_{mn}, for which λ_{11} and λ_{22} quantify the intraband coupling and λ_{12} and λ_{21} describe interband coupling. $H_{c2}(T)$ is described by a parametric equation[23]

$$\ln\frac{T}{T_{c0}} = -\left[U(h) + U\left(\frac{D_2}{D_1}h\right) + \frac{\lambda_0}{w}\right]\Big/2 + \left\{\left[U(h) - U\left(\frac{D_2}{D_1}h\right) - \frac{\lambda_-}{w}\right]^2\Big/4 + \frac{\lambda_{12}\lambda_{21}}{w}\right\}^{1/2},$$

$$U(h) = \psi(1/2+h) - \psi(1/2),$$

$$H_{c2} = 2\phi_0 k_B T h/\hbar D_1,$$

where $\psi(x)$ is the digamma function, ϕ_0 is the flux quantum, k_B is the Boltzmann constant, $\hbar$ is the Plank constant, $D_{1,2}$ are the anisotropic diffusivities of each band, and for H_{c2}^{ab}, the diffusivity D_1 should be replaced by $(D_1^{ab}D_1^c)^{1/2}$; $\lambda_- = \lambda_{11} - \lambda_{22}$, $\lambda_0 = (\lambda_-^2 + 4\lambda_{12}\lambda_{21})^{1/2}$, and $w = \lambda_{11}\lambda_{22} - \lambda_{12}\lambda_{21}$.

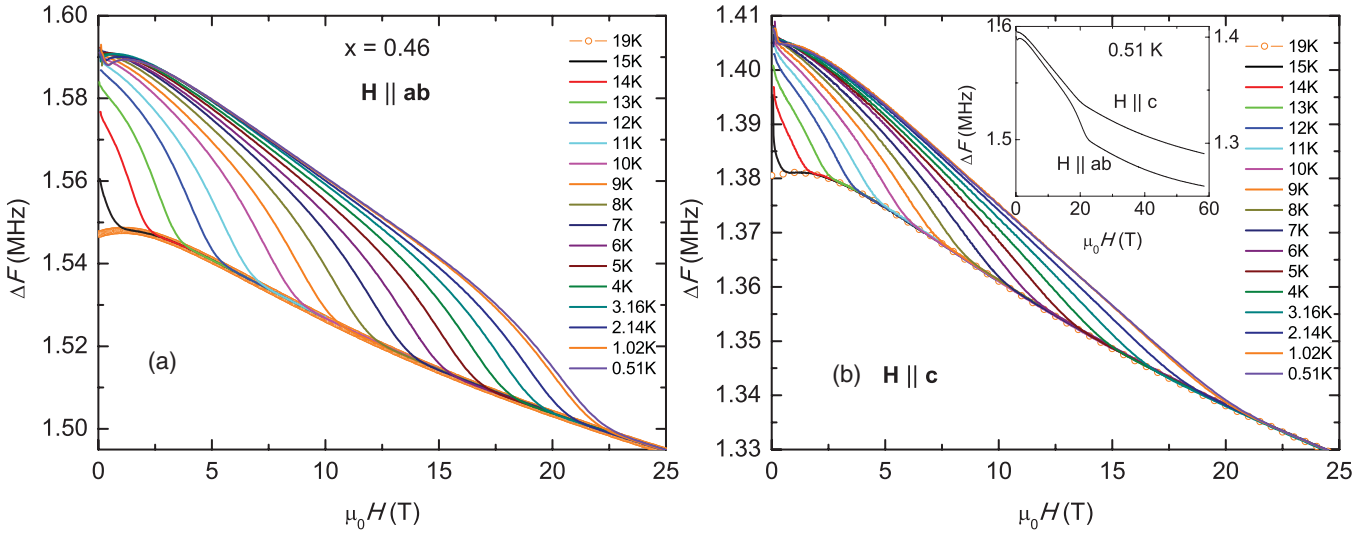

FIG. 3. (Color online) ΔF as a function of the magnetic field for $H \parallel ab$ and $H \parallel c$ for Eu46. The inset in (b) shows the measurements up to 60 T at the base temperature of 0.51 K.

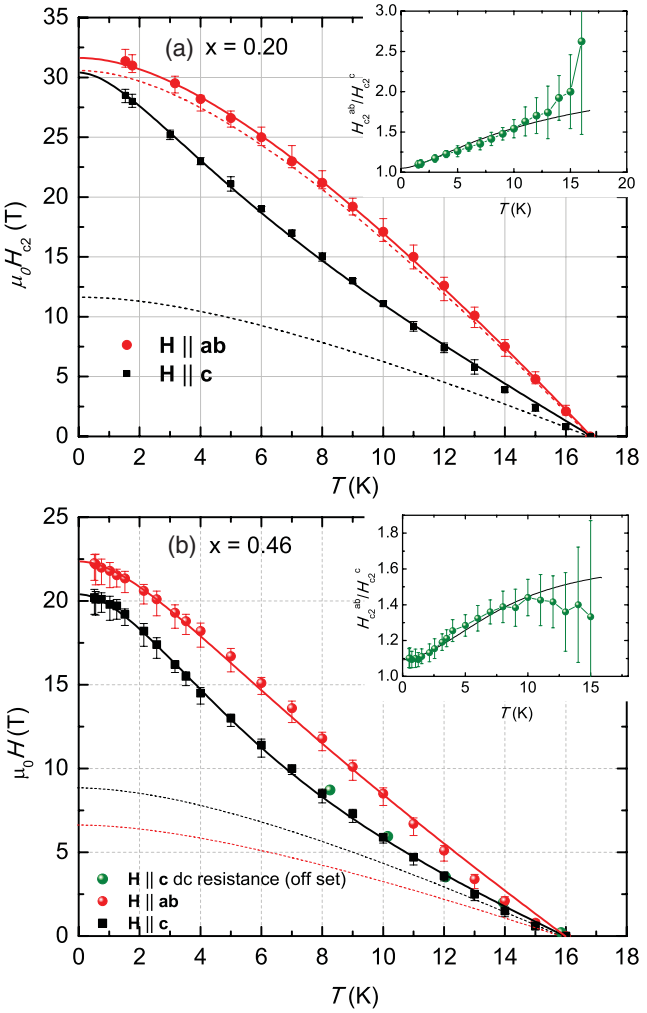

FIG. 4. (Color online) Anisotropic $H_{c2}(T)$ for Eu20 and Eu46 single crystals. The green circles in (b) are obtained from the resistivity measurement, which is in excellent agreement with the pulsed-field rf shift measurement. The dotted lines are fits to the WHH formula. The solid lines are fits to the two-band model. The insets show the temperature dependence of the anisotropy $\gamma = H_{c2}^{ab}/H_{c2}^{c}$, and the solid lines are the calculated curve of the two-band model fits.

Since only the product of λ_{12} and λ_{21} appears in the equation, we can assume that $\lambda_{12} = \lambda_{21}$. The fits to both $H_{c2}^{ab}(T)$ and $H_{c2}^{c}(T)$ for each sample are performed simultaneously in a self-consistent manner. The model fits the data remarkably well; it captures the main features of the $H_{c2}(T)$ curves. The fitting parameters are listed in Table I. In terms of diffusivity, the two bands exhibit strong asymmetry, i.e., the diffusivity ratio $\sqrt{D_2^{ab}D_2^{c}}/\sqrt{D_1^{ab}D_1^{c}} \sim 0.5$ and 0.2 for Eu20 and Eu46, respectively. Thus, superconductivity results from an anisotropic band with high diffusivity and a more isotropic band with smaller diffusivity. It should be noted that for the Eu20 sample, $H_{c2}^{c}(T)$ shows negative curvature, whereas $H_{c2}^{ab}(T)$ shows behavior similar to that which conforms with the conventional WHH theory. The two types of curvature for different field orientations have also been observed in $Ba(Fe_{0.93}Co_{0.07})_2As_2$.[24] But here we are describing both of them within the two-band model. For equal diffusivities of the two bands, i.e., $\eta = D_2/D_1 = 1$, the parametric equation of above reduces to the one-gap de-Gennes-Maki formula in the WHH theory, $\ln t + U(h) = 0$.[23] The diffusivity ratio of the Eu20 sample, $\eta^{ab} = D_2^{ab}/(D_1^{ab}D_1^{c})^{1/2}$ and $\eta^{c} = D_2^{c}/D_1^{c}$, is 0.77 and 0.11 for $H \parallel ab$ and $H \parallel c$, respectively. Therefore, it is reasonable to expect $H_{c2}^{ab}(T)$ with near unity η to show WHH-like behavior, in contrast to $H_{c2}^{c}(T)$ with much lower η and two-band-like behavior.

TABLE I. Parameters of the fits to the two-band model for $Sr_{1-x}Eu_x(Fe_{0.89}Co_{0.11})_2As_2$.

x	$\begin{pmatrix} D_1^{ab} & D_1^{c} \\ D_2^{ab} & D_2^{c} \end{pmatrix}$ (cm^2/s)	$\begin{pmatrix} \lambda_{11} & \lambda_{12} \\ \lambda_{21} & \lambda_{22} \end{pmatrix}$	$\mu_0 H_{c2}^{ab}(0)$ (T)	$\mu_0 H_{c2}^{c}(0)$ (T)	$\xi^{ab}(0)$ (nm)	$\xi^{c}(0)$ (nm)
0.20	$\begin{pmatrix} 0.16 & 1.35 \\ 0.36 & 0.15 \end{pmatrix}$	$\begin{pmatrix} 0.19 & 0.194 \\ 0.194 & 0.21 \end{pmatrix}$	31.6	30.4	3.3	3.2
0.46	$\begin{pmatrix} 0.79 & 2.27 \\ 0.28 & 0.25 \end{pmatrix}$	$\begin{pmatrix} 0.2 & 0.082 \\ 0.082 & 0.2 \end{pmatrix}$	22.4	20.4	4.0	3.7

The Eu20 sample shows strong interband pairing, i.e., $\lambda_{12}\lambda_{21} \simeq \lambda_{11}\lambda_{22}$, whereas the two bands become more noninteracting in the Eu46 sample, as indicated by $\lambda_{12}\lambda_{21} \ll \lambda_{11}\lambda_{22}$. It is noteworthy that the intraband pairing strength, λ_{11} and λ_{22}, remains almost unchanged for Eu concentration increases from 0.20 to 0.46; only the interband coupling decreases, with T_c decreasing slowly from 16.8 to 16 K. This observation may imply that superconductivity could be dominated by the intraband pairing and not be particularly sensitive to disorder and interband scattering. With the fitted values of $H_{c2}(T)$ at 0 K, we can estimate the anisotropic coherence length using $\xi^{ab} = \sqrt{\phi_0/2\pi H_{c2}^{c}}$ and $\xi^{c} = \phi_0/2\pi\xi^{ab}H_{c2}^{ab}$ (see Table I). Both ξ^{ab} and ξ^{c} are much larger than the spacing between the superconducting FeAs layers (~6 Å) in $Sr_{1-x}Eu_x(Fe_{0.89}Co_{0.11})_2As_2$, suggesting a three-dimensional (3D) characteristic of superconductivity.

The anisotropy of $H_{c2}(T)$ is plotted in the insets of Fig. 4. Both γ decrease with decreasing temperature, and approach 1 at zero temperature. It is qualitatively similar to that of the LiFeAs,[6] (Ba,K)Fe_2As_2,[4,11] and $LaFeAsO_{0.89}F_{0.11}$.[8] The isotropy of $H_{c2}(T)$ in FeAs superconductors with different carrier dopings is unexpected since distinctive hole and electron Fermi surfaces may be responsible for superconductivity with different dopings. For our Eu20 and Eu46 samples, there could be two factors contributing to the decreasing anisotropy: (i) at low temperature, band 2 with lower band anisotropy $D_2^{ab}/D_2^{c} \sim 2.4 - 1.1$ may become more important than band 1 with $D_1^{ab}/D_1^{c} \sim 0.12 - 0.35$; and (ii) the two bands have opposing anisotropy of diffusivity, i.e., for band 1, $(D_1^{ab}/D_1^{c}) < 1$, whereas for band 2, $(D_2^{ab}/D_2^{c}) > 1$. The calculated γ from the fits are shown as the solid lines in the insets. They well reproduce the temperature dependence of γ within error bars. Aside from the two-band model, another way of understanding the low-temperature approach to isotropy is by invoking the Pauli limit as the upper limit for both directions.

IV. CONCLUSIONS

To summarize, we measured the anisotropic $H_{c2}(T)$ for single crystals of $Sr_{1-x}Eu_x(Fe_{0.89}Co_{0.11})_2As_2$ ($x = 0.20$ and

0.46). Despite the presence of an Eu^{2+} moment, the Jaccarino-Peter effect is not observed up to 60 T at a base temperature of 0.5 K; it may be intrinsically absent in this system or a higher applied magnetic field may be needed. $H_{c2}(T)$ deviates from the WHH behavior as manifested by the upward curvature and is probably limited by Pauli paramagnetic pair breaking. The temperature dependence of $H_{c2}(T)$ is well described by a model of two bands with opposing anisotropy and large diffusivity difference. The $H_{c2}(T)$ becomes more isotropic at low temperature.

ACKNOWLEDGMENTS

This work was carried out at the Iowa State University and supported by the AFOSR-MURI Grant No. FA9550-09-1-0603 (R.H. and P.C.C.). Part of this work was performed at Ames Laboratory, US Department of Energy, under Contract No. DE-AC02-07CH 11358 (S.L.B. and P.C.C.). S.L.B. was also partially supported by the state of Iowa through the Iowa State University. Work at the NHMFL is supported by the NSF, the US Department of Energy, and the state of Florida.

*Present address: Center for Nanophysics, and Advanced Materials and Department of Physics, University of Maryland, College Park, Maryland 20742-4111, USA.

†Present address: Department of Physics, Mu'tah University, Mu'tah, Karak, 61710, Jordan.

[1] M. Shahbazi, X. L. Wang, C. Shekhar, O. N. Srivastava, Z. W. Lin, J. G. Zhu, and S. X. Dou, J. Appl. Phys. **109**, 07E162 (2011).

[2] C. Senatore, R. Flukiger, M. Cantoni, G. Wu, R. H. Liu, and X. H. Chen, Phys. Rev. B **78**, 054514 (2008).

[3] Xiaolin Wang, Shaban Reza Ghorbani, Germanas Peleckis, and Shixue Dou, Adv. Mater. **21**, 236 (2009).

[4] M. M. Altarawneh, K. Collar, C. H. Mielke, N. Ni, S. L. Bud'ko, and P. C. Canfield, Phys. Rev. B **78**, 220505(R) (2008).

[5] Mika Kano, Yoshimitsu Kohama, David Graf, Fedor Balakirev, Athena S. Sefat, Michael A. Mcguire, Brian C. Sales, David Mandrus, and Stanley W. Tozer, J. Phys. Soc. Jpn. **78**, 084719 (2009).

[6] J. L. Zhang, L. Jiao, F. F. Balakirev, X. C. Wang, C. Q. Jin, and H. Q. Yuan, Phys. Rev. B **83**, 174506 (2011).

[7] N. Ni, S. L. Bud'ko, A. Kreyssig, S. Nandi, G. E. Rustan, A. I. Goldman, S. Gupta, J. D. Corbett, A. Kracher, and P. C. Canfield, Phys. Rev. B **78**, 014507 (2008).

[8] F. Hunte, J. Jaroszynski, A. Gurevich, D. C. Larbalestier, R. Jin, A. S. Sefat, M. A. McGuire, B. C. Sales, D. K. Christen and D. Mandrus, Nature (London) **453**, 903 (2008).

[9] J. Jaroszynski, F. Hunte, L. Balicas, Youn-jung Jo, I. Raicevic, A. Gurevich, D. C. Larbalestier, F. F. Balakirev, L. Fang, P. Cheng, Y. Jia, and H. H. Wen, Phys. Rev. B **78**, 174523 (2008).

[10] S. A. Baily, Y. Kohama, H. Hiramatsu, B. Maiorov, F. F. Balakirev, M. Hirano, and H. Hosono, Phys. Rev. Lett. **102**, 117004 (2009).

[11] H. Q. Yuan, J. S. ingleton, F. F. Balakirev, S. A. Baily, G. F. C. hen, J. L. Luo, and N. L. Wang, Nature (London) **457**, 565 (2009).

[12] Rongwei Hu, Sergey L. Bud'ko, Warren E. Straszheim, and Paul C. Canfield, Phys. Rev. B **83**, 094520 (2011).

[13] V. Jaccarino and M. Peter, Phys. Rev. Lett. **9**, 290 (1962).

[14] ø Fischer, M. Decroux, S. Roth, R. Chevrel, and M. Sergent, J. Phys. C **8**, 474 (1975).

[15] H. W. Meul, C. Rossel, M. Decroux, O. Fischer, G. Remenyi, and A. Briggs, Phys. Rev. Lett. **53**, 497 (1984).

[16] C. Mielke, J. Singleton, M.-S. Nam, N. Harrison, C. C. Agosta, B. Fravel, and L. K. Montgomery, J. Phys. Condens. Matter **13**, 8325 (2001).

[17] T. Coffey, Z. Bayindir, J. F. DeCarolis, M. Bennett, G. Esper, and C. C. Agosta, Rev. Sci. Instrum. **71**, 4600 (2000).

[18] M. M. Altarawneh, C. H. Mielke, and J. S. Brooks, Rev. Sci. Instrum. **80**, 066104 (2009).

[19] Amikam Aharoni, J. Appl. Phys. **83**, 3432 (1998).

[20] E. D. Mun, M. M. Altarawneh, C. H. Mielke, V. S. Zapf, R. Hu, S. L. Bud'ko, and P. C. Canfield, Phys. Rev. B **83**, 100514(R) (2011).

[21] N. R. Werthamer, E. Helfand, and P. C. Hohenberg, Phys. Rev. **147**, 295 (1966).

[22] A. M. Clogston, Phys. Rev. Lett. **9**, 266 (1962).

[23] A. Gurevich, Phys. Rev. B **67**, 184515 (2003).

[24] V. A. Gasparov, L. Drigo, A. Audouard, D. L. Sun, C. T. Lin, S. L. Bud'ko, P. C. Canfield, F. Wolff-Fabris, and J. Wosnitza, JETP Lett. **93**, 667 (2011).